JOURNAL OF GEOPHYSICAL RESEARCH, VOL. 106, NO. A9, PAGES 18,763–18,775, SEPTEMBER 1, 2001

Role of the magnetosheath flow in determining the motion of open flux tubes

B. M. A. Cooling

Astronomy Unit, Queen Mary, University of London, London, England

C. J. Owen

Mullard Space Science Laboratory, University College London, University of London, London, England

S. J. Schwartz

Astronomy Unit, Queen Mary, University of London, London, England

Abstract. We have constructed a model which examines the motion of reconnected magnetic flux tubes over the surface of the magnetopause. For a given interplanetary magnetic field (IMF) we first determine the draping and strength of the magnetosheath magnetic field, flow velocity, and density over the entire surface of a paraboloid magnetopause. For a given magnetopause location we apply a test for steady state reconnection occurring between the magnetosheath field and a modeled magnetospheric field at that point. We trace the subsequent motion of these tubes along the surface of the magnetopause and into the magnetotail. Results are shown for a range of cases. The model has applications in testing various hypotheses about the location of reconnection events and, for example, IMF B_Y effects. In particular, it highlights the dominance of the magnetosheath flow model in determining the motion of the tubes and the necessity of sub-Alfvénic magnetosheath flows for the occurrence of steady state reconnection poleward of the cusp during periods of northward IMF. Our model may also be used to identify likely reconnection sites on the dayside and near-Earth nightside magnetopause and to identify possible locations for steady state reconnection.

1. Introduction

Dungey [1961] introduced the idea of magnetic reconnection as a mechanism for imparting solar wind energy into the Earth's magnetosphere. There has been much observational evidence in support of Dungey's idea [e.g., *Sonnerup et al.*, 1981; *Gosling et al.*, 1982, 1986]. Stress balance calculations for reconnecting field lines based on the simple classical case of southward B_Z interplanetary magnetic field (IMF) reconnecting at the subsolar point with an antiparallel geomagnetic field line, lead to the conclusion that plasma jets in the magnetopause boundary layer, thought to be signatures of reconnection, should have speeds of $\sim 2V_A$ [*Sonnerup*, 1979; *Cowley*, 1979, 1981]. Reconnection at arbitrary angles has also been considered. *Petschek* [1964] noted that an arbitrary magnetic field component in the direction of the reconnection line may be added without changing the validity of the analysis, and observational signatures support this view. For example, pure north/south jetting of the earlier simple models is modified in the presence of IMF B_Y (dawn-dusk) components. A range of B_Y asymmetries have been identified [e.g., *Svalgaard*, 1968; *Mansurov*, 1969; *Heppner*, 1972; *Cowley*, 1981; *Cowley et al.*, 1983].

In recent years, attention has been focused on reconnection other than at the subsolar dayside magnetopause, in particular for cases of northward IMF poleward of the cusps. Opinion is divided on whether steady state reconnection is achievable under these conditions [*Rodger et al.*, 2000].

In an attempt to address some of these issues theoretically, *Cowley and Owen* [1989] (hereinafter referred to as CO89) developed a simple model to illustrate the initial motion of flux tubes created by reconnection between magnetic fields of equal strength but arbitrary orientation across a planar magnetopause. This study has been useful in investigating a number of aspects of dayside reconnection where a qualitative and quantitative framework is needed. For example, *Lockwood* [1997] used CO89 to model the energy and pitch angle dispersions of low-latitude boundary layer (LLBL) /cusp ions and estimated from such kinetic observations the Alfvén speed and field-aligned flow at the magnetopause reconnection site [*Lockwood*, 1995]. The model has been used to demonstrate that both the acceleration of cold ion beams [*Gosling et al.*, 1990] and the spectra of par-

Paper number 2000JA000455.
0148-0227/01/2000JA000455$09.00

ticles crossing the magnetopause and in the cusp/cleft region [*Lockwood and Smith*, 1994; *Onsager et al.*, 1995] may be accounted for in terms of reconnection events.

CO89 has also been used in looking at global flow patterns and currents. Predictions based on this model have been compared to observations of inflow and outflow (boundary layer) velocities of particles following reconnection events [*Song and Russell*, 1992; *Mei et al.*, 1995; *Chen et al.*, 1997; *Siscoe et al.*, 2000]. The model supports the view that low- and high-latitude cleft currents are not extensions of Region 1 and Region 2 current systems but arise from newly reconnected field lines on the dayside magnetopause [*Taguchi et al.*, 1993]. *Korotova and Sibeck* [1995], *Rodger et al.* [2000], and *Coleman et al.* [2000] have made use of the model in determining whether reconnection events are steady state or transient. *Lockwood and Smith* [1994] and *Lockwood and Davis* [1995] have used it to demonstrate that neither the spectra of particles crossing the magnetopause nor flux line evolution are significantly affected by the reconnection rate.

A third area in which the CO89 model has proved useful is in considering mechanisms by which mass, energy, and momentum enter the magnetosphere. For example, *Owen and Cowley* [1991] used it to evaluate *Heikkila's* [1982] impulsive transport mechanism. *Konik et al.* [1994] investigated how the orientation of the IMF affects magnetic impulse events [*Konik et al.*, 1994]. *Drakou et al.* [1994] used the model to explain the assimilation of reconnected flux tubes under northward IMF into the magnetosphere.

The CO89 model is, however, too restrictive for many applications. It deals with a planar magnetopause and employs simplified representations of the magnetic fields and sheath flow. Some studies have addressed these points by using, for example, *Tsyganenko's* [1995] magnetopause description, [e.g., *Rodger et al.*, 2000], or by using some form of magnetosheath field draping, [e.g., *Lockwood*, 1995, 1997; *Rodger et al.*, 2000].

In this paper we present a simple model which extends the work of CO89 by including components which account for (1) draping of the magnetic fields at a more realistic magnetopause; (2) an improved model for magnetosheath flow; (3) where and whether reconnection may occur; (4) stress balance on reconnecting field lines; and (5) predictions of the subsequent long-term evolution of the flux tube motion.

In section 2 we outline the components of the model and assumptions we have made. In section 3 we present several case studies showing the predictions from the model. Examples with southward IMF behave as expected on the basis of the present understanding of subsolar reconnection. We show that steady state reconnection poleward of the cusps under northward IMF may only be achieved by modifying the parameters of the model so that the magnetosheath flow becomes sub-Alfvénic in these regions. We also show that "toward"/"away" Parker spiral directions result in asymmetric motion of reconnected flux tubes about the noon meridian. Such asymmetry has consequences for convection inside the magnetosphere and at the footpoints of the reconnected flux tubes in the auroral ionosphere. Finally, in section 4 we discuss and summarize our findings.

2. Model Development

In this section we first outline the scheme of our model and its component parts. Next we discuss those parts of our model directly derived from CO89, i.e., the stress balance of two reconnecting field lines and the instantaneous motion of the open flux tubes. We then describe how we integrate that motion to determine trajectories of reconnected flux tubes over the magnetopause surface. We develop the models which we have used for the magnetosheath [*Kobel and Flückiger*, 1994] and geomagnetic fields, the sheath flow speed, and the density immediately adjacent to the magnetopause [*Spreiter et al.*, 1966]. Lastly, we formulate our initial reconnection test and how we establish a merging line and the steady state reconnection test which we apply.

2.1. Scheme

Figure 1 shows the flow diagram of our model. We specify the solar wind velocity and the IMF strength and direction, the bow shock and magnetopause standoff distances, and a location for reconnection. This information feeds through to the magnetosheath flow and density models and to the magnetopause magnetic field models. The sheath flow speed, density, and components of the magnetic field on either side of the magnetopause at the proposed location are then calculated. Next, a test for the possibility of initial reconnection is carried out. If the test is satisfied, the length and orientation of a merging line are determined. Initial velocities of reconnected field lines are calculated from the balance of field and plasma stresses on these field lines, and a test for steady state reconnection is applied. The velocities of a number of representative flux tubes in the Earth frame are calculated, and their positions are incremented over a short time interval. The new locations are fed back into the model, and the magnetosheath flow, the density, the fields, and the stress balance conditions at the new points are calculated. The locations of the intersection of these open flux tubes with the magnetopause may thus be determined over a desired time interval. In essence, we are quantifying the process illustrated by *Crooker* [1979], and elements of this approach are similar to those described by *Lockwood* [1997].

2.2. Stress Balance

At the magnetopause we define a local orthogonal coordinate system $\hat{\mathbf{q}}$, $\hat{\mathbf{j}}$, $\hat{\mathbf{n}}$ such that $\hat{\mathbf{q}}$ is tangential to the current sheet and parallel to the direction $\mathbf{B}_{ms} - \mathbf{B}_{gm}$, where $\mathbf{B}_{ms}$ and $\mathbf{B}_{gm}$ are the draped magnetosheath and geomagnetic fields either side of the magnetopause respectively; $\hat{\mathbf{j}}$ is also tangential to the local magnetopause current sheet and parallel to the current, i.e., in the direction $\nabla \wedge \mathbf{B}$; and $\hat{\mathbf{n}}$ is the outward normal to the local current sheet. In this system, magnetic fields $\mathbf{B}_{ms}$ and $\mathbf{B}_{gm}$ either side of the sheet may be written as (B_{msq}, B_j, B_n) and (B_{gmq}, B_j, B_n), so both the $\hat{\mathbf{j}}$ and $\hat{\mathbf{n}}$ components of the field remain constant across

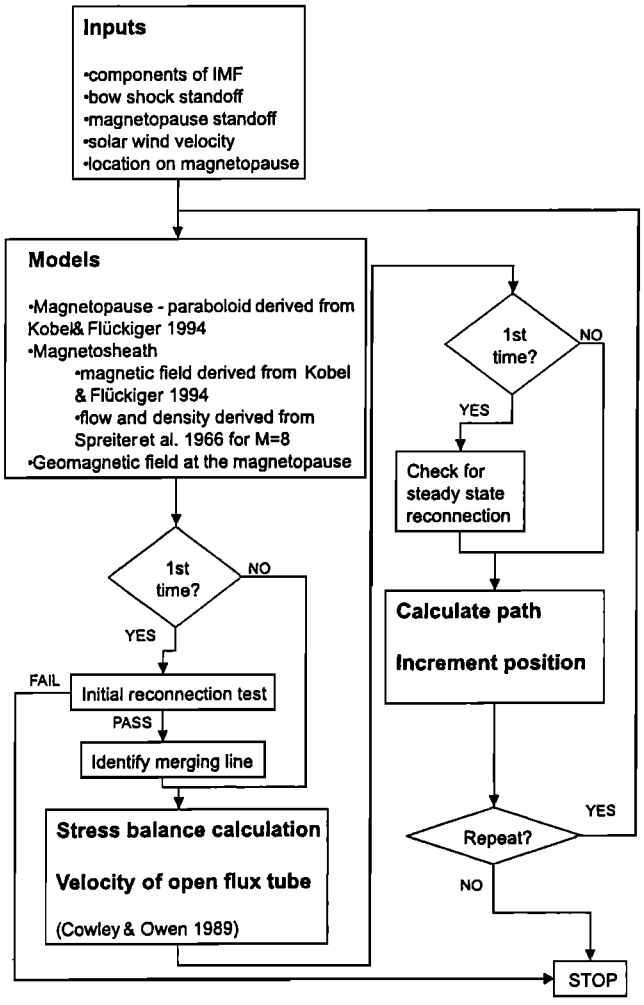

Figure 1. Flow diagram of the model operations developed in the study. We input the solar wind velocity, the interplanetary magnetic field (IMF), bow shock and magnetopause standoff distances, and a location to attempt to initiate reconnection. Initial reconnection tests are carried out, and if successful the model calculates the relevant plasma parameters, calculates the flux tube velocity, and increments the position. Calculations are repeated at the new location, and the process is repeated for the desired time interval. The trace of the intersection of the open flux tube with the magnetopause is plotted over the desired time interval.

the magnetopause. Here $B_n \neq 0$ for a rotational discontinuity, or open magnetopause. We can find a *de Hoffmann and Teller* [1950] (hereinafter referred to as dHT) frame in which the local convection electric field is transformed away, such that in this frame the plasma flows along the field direction, i.e., $\mathbf{V} \wedge \mathbf{B} = \mathbf{0}$. We make the additional assumption that the flow is dominated by the magnetosheath plasma moving into the magnetosphere.

We assume that we are working with a rotational discontinuity in an isotropic MHD plasma. Following the calculations of *Parks* [1991] and CO89 we arrive at the result:

$$V^2 = \frac{B^2}{\mu_0 \rho} = {V_A}^2, \tag{1}$$

where V is the field-aligned inflow and outflow speed of the plasma and V_A is the Alfvén speed of the system.

The sheath and boundary layer plasmas have the same density and field strength as a consequence of the assumption that the plasma is isotropic and is a pure rotational discontinuity across a simple, single-layered, thin current sheet. It is much more likely, however, that it is comprised of multiple layers and is possibly better described as a standing wave structure [*Cowley*, 1995]. Here we consider the changes encountered by plasma entering the magnetosphere via a reconnection mechanism only across the outermost layer of the magnetopause consisting of an Alfvén wave (or rotational discontinuity). The Alfvén wave acts only to rotate the magnetic field direction and accelerate the particles in this model. It does not affect the thermodynamic properties of the plasma [*Cowley*, 1995].

2.3. Flux Tube Motion

2.3.1. Instantaneous flux tube velocity along the magnetopause. Following reconnection, the reconfigured magnetic fields divide into two separate open flux tubes. The velocities calculated from stress balance in section 2.2 are those in the dHT or field line rest frame. The velocity space diagram in Figure 2 illustrates the relationship between the velocity vectors in the dHT frame and those in the Earth frame.

The frame transformation velocities described in Figure 2 are simply the differences between the flow velocities as measured in the two frames, i.e.,

$$\mathbf{V}_{HTN} = \mathbf{V}_{sh} - V_A \mathbf{b}_{ms}, \tag{2}$$

$$\mathbf{V}_{HTS} = \mathbf{V}_{sh} + V_A \mathbf{b}_{ms}. \tag{3}$$

The boundary layer (outflow) velocities on the magnetospheric side are

$$\mathbf{V}_{gmN} = \mathbf{V}_{HTN} + V_A \mathbf{b}_{gm}, \tag{4}$$

$$\mathbf{V}_{gmS} = \mathbf{V}_{HTS} - V_A \mathbf{b}_{gm}, \tag{5}$$

which become

$$\mathbf{V}_{gmN} = \mathbf{V}_{sh} + V_A(\mathbf{b}_{gm} - \mathbf{b}_{ms}), \tag{6}$$

$$\mathbf{V}_{gmS} = \mathbf{V}_{sh} - V_A(\mathbf{b}_{gm} - \mathbf{b}_{ms}). \tag{7}$$

At the subsolar point where $V_{sh} = 0$ (6) and (7) give boundary layer outflow speeds of just $2V_A$ for antiparallel fields as expected [*Crooker*, 1979].

2.3.2. Integrated flux tube motion. Once we have calculated the velocity $\mathbf{V}_{HT}$ of a particular tube along the magnetopause, we then increment the position vector by $\mathbf{V}_{HT}\Delta T$, where ΔT is a short time interval. The new position is constrained to lie on the magnetopause by projection along the local normal.

The plasma and field parameters at the new location are determined in order to calculate the new flux tube velocity and perform a second incrementation of flux tube position.

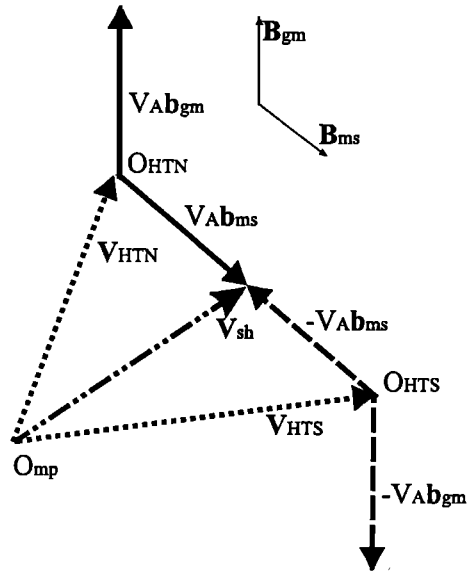

Figure 2. Velocity space diagram illustrating the relationship between the various velocity vectors following reconnection at an arbitrary point. The magnetosheath and geomagnetic field vectors, labeled $\mathbf{B}_{ms}$ and $\mathbf{B}_{gm}$, respectively, are shown in the top right of Figure 2. The dot-dashed line labeled $\mathbf{V}_{sh}$ shows the magnetosheath flow in the Earth rest frame. Following reconnection, a pair of open flux tubes is formed connected to the northern and southern cusps, respectively. In the reconnected field line rest frame (dHT) for each tube, which have origins O_{HTN} and O_{HTS}, the sheath flow appears as a field-aligned flow at the Alfvén speed. This is indicated by the thick solid arrow marked $V_A\mathbf{b}_{ms}$ for the flux tube connected to the northern cusp and by the thick dashed line marked $-V_A\mathbf{b}_{ms}$ for the flux tube connected to the southern cusp. Consequently, the instantaneous flux tube motions can be constructed and are indicated by the dotted vectors marked $\mathbf{V}_{HTN}$ and $\mathbf{V}_{HTS}$, respectively. Plasma in the magnetospheric boundary layer is also moving at the Alfvén speed along the geomagnetic field line in the dHT frame, represented by vectors marked $V_A\mathbf{b}_{gm}$ and $-V_A\mathbf{b}_{gm}$, respectively.

This process is repeated as required in order to determine the trajectory of each flux tube along the magnetopause surface.

In our model we assume that the path followed by the flux tube moves only under the magnetic tension $\mathbf{j} \wedge \mathbf{B}$ forces. However, in addition to the rotational discontinuity there may be fast or other disturbances which influence motion, especially far from the reconnection site, which we ignore.

2.4. Coordinate System

In defining the global aspects of the model, such as the magnetic fields and sheath flow parameters, we use a right-handed orthogonal system, X, Y, Z, based on GSM coordinates. The origin is based at the center of the Earth; the X axis lies along the Sun-Earth axis (positive X is toward the Sun); positive Y points toward dusk; and the Z axis, representing the dipole axis, is aligned south to north. In this initial study we neglect the effects of dipole tilting.

2.5. Magnetic Field Models

2.5.1. Magnetosheath Field. On passing through the bow shock the solar wind plasma is slowed and deflected in order to pass around the magnetosphere. As a consequence of the frozen-in flux theorem, the magnetic field in the magnetosheath initially drapes around the geomagnetic field, forming a tangential discontinuity at the magnetopause [e.g., *Crooker et al.*, 1985]. We use the analytical model of *Kobel and Flückiger* [1994] (hereinafter referred to as KF94) as the basis for deriving the magnetosheath field just outside the magnetopause.

The KF94 model requires only three inputs: the standoff distances of the bow shock, R_{bs}, and magnetopause, R_{mp}, from the Earth's center, and the IMF components B_{imfX}, B_{imfY}, and B_{imfZ}.

The bow shock and the magnetopause are each described as paraboloids of revolution about the X- axis with foci midway between the Earth and the subsolar point. In our coordinate system the magnetopause surface is defined as

$$Y^2 + Z^2 = 2R_{mp}(R_{mp} - X). \tag{8}$$

This model compares well with others [see *Elsen and Winglee*, 1997] out to $X \sim -20$ to -30 R_E where the radius of the magnetopause is ~ 25 R_E. Other models tend to become more cylindrical downtail, reaching a radius of 25 R_E at $X \sim -100$ R_E.

The field within the magnetosheath is assumed to be current-free [e.g., *Fairfield*, 1979] except at the outer and inner boundaries. Potentials are then matched at the boundaries to arrive at a description of the field at any point within the magnetosheath. We applied this model to determine the components B_{msX}, B_{msY}, and B_{msZ} of the magnetosheath field at a given location (X, Y, Z) immediately outside the magnetopause boundary. These are given by

$$B_{msX} = -A[-B_{imfX}(1 - \frac{R_{mp}}{2l}) + B_{imfY}(\frac{Y}{l}) + B_{imfZ}(\frac{Z}{l})], \tag{9}$$

$$B_{msY} = A[-B_{imfX}(\frac{Y}{2l}) + B_{imfY}(2 - \frac{Y^2}{lR_{mp}}) - B_{imfZ}(\frac{YZ}{lR_{mp}})], \tag{10}$$

$$B_{msZ} = A[-B_{imfX}(\frac{Z}{2l}) - B_{imfY}(\frac{YZ}{lR_{mp}}) + B_{imfZ}(2 - \frac{Z^2}{lR_{mp}})], \tag{11}$$

where

$$A = \frac{2R_{bs} - R_{mp}}{2(R_{bs} - R_{mp})}, \tag{12}$$

where typically, $A = 2$ and l is the distance from the focus to the magnetopause surface:

$$l = \frac{3R_{mp}}{2} - X. \tag{13}$$

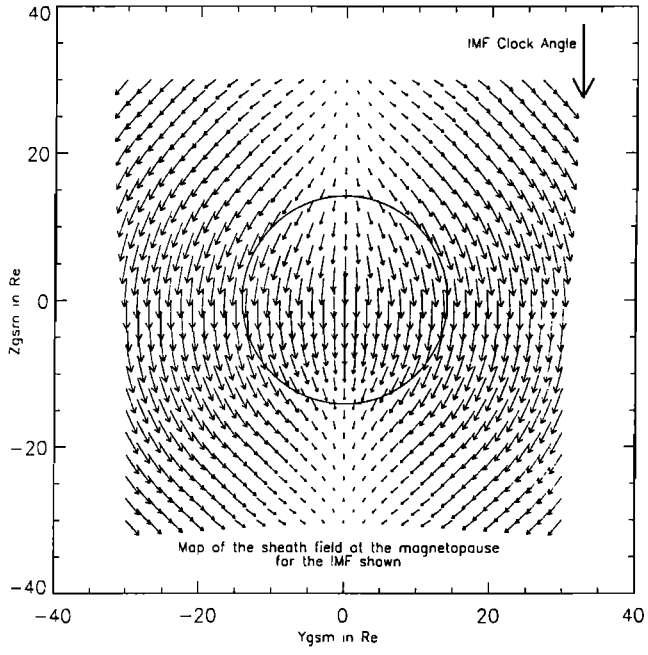

Figure 3. The projection of the unreconnected draped magnetosheath field resulting from pure southward IMF just outside the magnetopause. Figure 3 is drawn looking down the X axis from the Sun with the Y (dawn-dusk) coordinate along the horizontal axis and the Z (south-north) coordinate along the vertical axis. The large arrow in the top right-hand corner indicates the projection of the IMF direction. The short arrows show the Y and Z components of the magnetosheath field vector calculated from the KF94 model. The superimposed circle has the radius of $\sim 15\ R_E$which is the radius of the magnetopause at $X = 0$. Draping of the field in the $\pm Y$ - direction as we move away from the origin is clearly seen. Draping in the X direction also occurs.

Equations (9) - (13) are valid only on the paraboloid surface defined by l. The general equations from which they are derived are curl-free. The normal component of the curl of (9) - (13) is also zero.

Apart from its analytical nature, a major feature of this model is that unlike other models [e.g., *Alksne*, 1967] based on gasdynamic considerations, it does not give an infinite magnitude for the magnetosheath field at the subsolar point. This model also allows for draping in three- dimensions. Figure 3 shows the YZ plane projection of the draped magnetosheath field just outside the magnetopause for a pure southward IMF prior to reconnection. As we move away from the $Y = 0$ and $Z = 0$ axes, draping in the Y direction can be clearly seen in Figure 3, becoming more pronounced as Y increases. Draping in the X direction also occurs. The clock angle of the IMF is clearly not preserved. The equivalent result for pure northward IMF (not shown) is a reflection of Figure 3 about $Z = 0$.

2.5.2. Geomagnetic field at the magnetopause boundary. From the simplifying assumptions of our stress balance calculations, we obtain the result that the magnetic field strength of the reconnected field line is equal on both sides of the current sheet during all stages. For this reason we require only the direction of the magnetospheric field just inside the magnetopause boundary. Additionally, we are constrained to use a paraboloid model by our choice of the KF94 magnetosheath field model. We consider therefore that the use of a more detailed geomagnetic field model, such as that of *Tsyganenko* [1995], is not warranted at this stage of our work.

We have modeled the unperturbed geomagnetic field at the inner edge of the magnetopause boundary very simply, on the basis of the following assumptions: The direction of the field prior to reconnection is everywhere tangential to the magnetopause. We place the cusps on the magnetopause at the locations $(1/2\ R_{mp}, 0, \pm R_{mp})$. All field lines map from the southern to the northern cusp over the surface of the paraboloid. In XY projection the field lines map in straight lines from any point on the surface toward the northern cusp and away from the southern cusp. Figure 4 shows the mapping of the assumed geomagnetic field onto the YZ plane prior to reconnection. Note that special treatment is required if the fields at the singular cusp points are needed. In this case the geomagnetic field vector is pointed directly toward or away from the relevant geographical pole, and the field strength is zero.

2.6. Sheath Flow and Density

In order to calculate the flux tube motion we also require a model for the magnetosheath flow velocity at locations adjacent to the magnetopause. One of the most commonly used models in this area [e.g., *Mei et al.*, 1995; *Lockwood*, 1997],

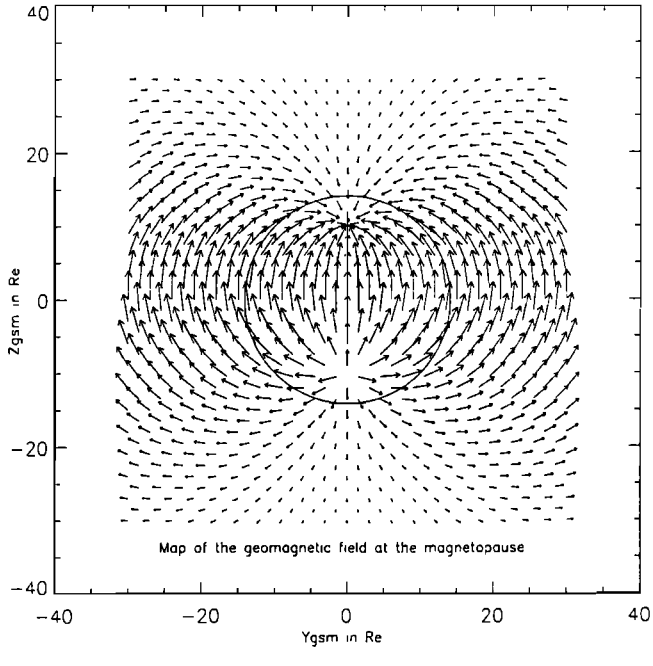

Figure 4. Similar to Figure 3 but showing the YZ projection of the unreconnected geomagnetic field just inside the magnetopause boundary. The southern cusp at $(5, 0, -10)R_E$ shows clearly as a "source", and the northern cusp at $(5, 0, 10)R_E$ shows clearly as a "sink" for the magnetic field lines in this model.

is that of *Spreiter et al.* [1966], based on simulation studies of gasdynamic flow around an obstacle. Assuming cylindrical symmetry, we have fitted a magnetosheath flow speed variation at the magnetopause, $V(X)$, to *Spreiter et al.'s* [1966] result for solar wind with fast magnetosonic Mach number 8 and $\gamma = 5/3$ by the curve:

$$\frac{V(X)}{V_{sw}} = 0.784 \ln(1 + \sqrt{\frac{2(R_{mp} - X)}{R_{mp}}}), \qquad (14)$$

where V_{sw} is the velocity of the unshocked solar wind. The projection of this flow vector on the YZ plane (not shown) is directed radially away from the stagnation point. This ratio reaches 1 for $X \sim -23\ R_E$.

The density at the magnetopause was also derived from *Spreiter et al.* [1966] and fitted by

$$\frac{\rho(X)}{\rho_{sw}} = 1.509 \exp(\frac{X}{R_{mp}}) + 0.1285, \qquad (15)$$

where ρ_{sw} is the density of the unshocked solar wind. This ratio has a maximum value of 4.23 at the subsolar point. Once more, the simplifying assumptions of section 2.2 imply that the densities of the reconnecting plasmas immediately either side of the magnetopause on a given pair of reconnected field lines are the same in this model.

While the geometry of *Spreiter et al.'s* [1966] magnetopause model differs from that of KF94, the latter claim good qualitative agreement between the streamline patterns found in the two models. The individual components of our model are all representative and allow easy manipulation. Additionally, the high degree of symmetry in the model field and flow configuration enables the control by the IMF to be unambiguously defined.

2.7. Reconnection Conditions

Many aspects of reconnection remain the subject of debate. In particular, the conditions leading to the occurrence of reconnection at a given point are unknown, as are the parameters controlling the length and orientation of the merging line. Moreover, it appears that reconnection may occur as a quasi-steady state process, or a sporadic, time-dependent process, for example, flux transfer events [*Russell and Elphic*, 1979; *Korotova and Sibeck*, 1995; *Onsager et al.*, 1995]. In this work we make a number of ad hoc assumptions concerning these factors. Our model includes an initial reconnection test, an algorithm to put limits on the length of a merging line, and a test of whether reconnection can proceed in a steady state manner. Each of these tests is described below.

2.7.1. Initial reconnection test. There are various hypotheses as to where and under what conditions reconnection may occur. Reconnection may simply occur if there are antiparallel components perpendicular to the merging line [e.g., *Gonzalez and Mozer*, 1974; *Luhmann et al.*, 1984]. Alternatively, reconnection may be restricted to occur only where the magnetosheath and geomagnetic fields are exactly antiparallel [e.g., *Crooker*, 1979]. Other hypotheses assume that reconnection may occur if the mean current density is great enough to cause anomalous resistivity [e.g., *Pudovkin and Semenov*, 1985].

In our model we input a location for reconnection. We check that the draped magnetosheath and geomagnetic fields are not exactly parallel, and we apply the threshold criterion to the magnitude of the difference in components perpendicular to the current direction (i.e., $|\Delta B_q|$) above which reconnection is allowed to occur (where $|\Delta B_q|$ serves as a proxy for the mean current density in the sheet).

In practice, this test will allow reconnection for any shear angle provided that the strength of the components is great enough. For lower field strengths a larger shear angle is required before reconnection may proceed. Even if the shear angle is 180°, reconnection may not proceed if the strengths of the perpendicular field components are too weak. This is illustrated in Figure 5 in which shaded contours represent shear angle resulting from a typical Parker spiral IMF with a moderately strong southward B_Z component of 6 nT. Threshold values of 35 and 50 nT corresponding to magnetopause currents of 28 and 40 $mA\ m^{-1}$, respectively, are overplotted. Reconnection will occur provided the threshold test is satisfied at the chosen location. So, for example, in Figure 5, for a threshold of 50 nT, reconnection may occur if the selected position is within the central band stretching from the top left of the figure to the bottom right. Figures similar to Figure 5 may be produced for any IMF and used as an aid for selection of an appropriate location for initial reconnection. In Figure 5, for example, we would therefore favor initial locations in the two white bands between the 50

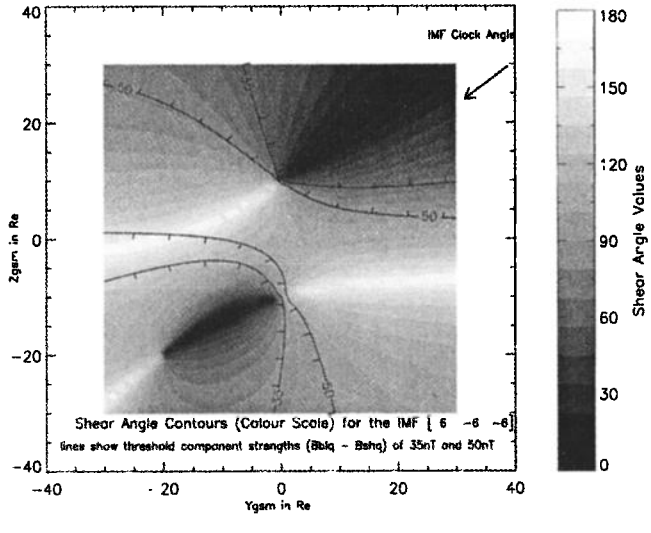

Figure 5. Contours of the shear angle between the magnetosheath and magnetosphere fields at the magnetopause shown in gray scale for the Parker spiral IMF with $-B_Z$, $(6, -6, -6)$nT. Lines showing thresholds ($|\Delta B_q|$ as described in the text) of 35 and 50 nT are overplotted. Note that in practice, there are areas where even with antiparallel magnetic fields, the threshold test may fail for weak field strengths, and that there are areas of lower shear angle where it may succeed for strong fields.

nT contours. In our examples we use a threshold of 35 nT. This is an arbitrary choice, designed to allow reconnection at the subsolar point for a pure southward IMF of 5 nT or more.

2.7.2. Merging line. The existence or otherwise of a merging line and its orientation are also open questions. *Gonzalez and Mozer* [1974] propose a merging line lying along the direction in which the magnetosheath and geomagnetic fields have equal parallel components (in effect, the magnetopause current direction) and extending globally along the magnetopause, not necessarily passing through the subsolar point [*Gonzalez*, 1991].

Crooker has developed various models, one insisting that the merging line passes through the cusps [e.g., *Crooker*, 1979] and another through the subsolar point [e.g., *Crooker et al.*, 1990]. A further model [*Crooker*, 1985] suggests a split-separator merging line derived from *Stern* [1973], who proposed that a separator line in a uniform field plus dipole (modeling the geomagnetic field) will split into two separate lines in the presence of surface currents.

In our model we calculate the direction of the reconnection current at a location and assign this as the merging line. Using, say, a Tsyganenko 96 model for the geomagnetic field would change the direction slightly but would not be consistent with the reconnection model employed here. The model increments along the local current direction until the threshold test, described in section 2.7.1, fails, up to an arbitrary maximum length.

Determining the length and orientation of the merging line is not a key feature of our model. In our examples we have used a maximum length of 8 R_E though, in fact, the merging line may be much longer.

2.7.3. Steady state reconnection. When magnetic fields reconnect, two flux tubes are formed which must peel away from the merging line on opposite sides (CO89). If this is not the case, the tubes would have to cross back over the merging line, which implies a temporal evolution at the reconnection site. We test that the components of the two flux tube velocities perpendicular to the merging line are in opposite directions. Using (2) and (3), this condition may be stated as

$$| \mathbf{V}_{sh}.\hat{\mathbf{q}} | < | V_A \mathbf{b}_{ms}.\hat{\mathbf{q}} | , \qquad (16)$$

from which it may be seen that the ratio of the magnetosheath flow speed to the Alfvén speed (CO89) is particularly important.

3. Results

In this section we describe a number of representative examples of the output from our model. We ran each of the examples using the following parameters: R_{bs} = 15 R_E, R_{mp} = 10 R_E, V_{sw} = 400 $km\ s^{-1}$, n_{sw} = 10 cm^{-3}; we also assume that the ion population is composed entirely of protons. We impose an initial reconnection threshold magnetic field strength of 35 nT (see Section 2.7.1), and a maximum merging line length of 8 R_E (see Section 2.7.2). We iterate reconnected flux tube motion over a time step $\Delta T = 0.5s$ for a total duration of 500 s.

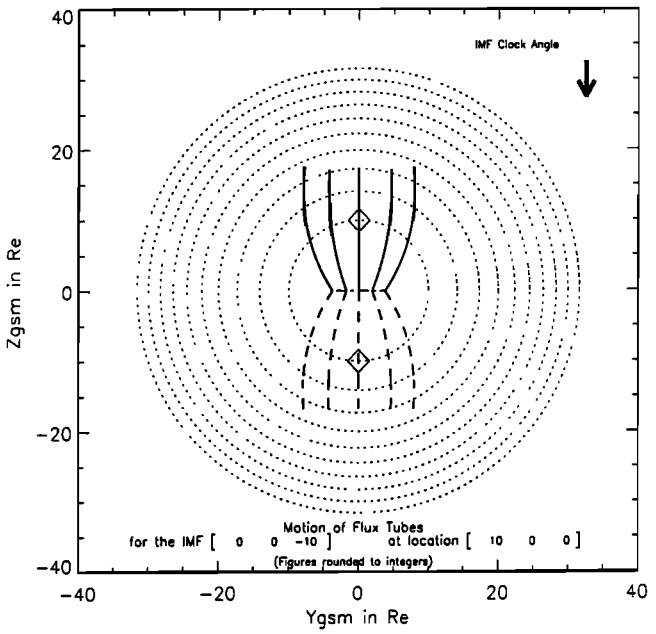

Figure 6. Motion of reconnected flux tubes for subsolar reconnection under pure southward IMF. Figure 6 is projected in the YZ plane, looking earthward from the Sun. The dotted circles indicate the radius of the magnetopause at X coordinate intervals of 5 R_E. The innermost circle represents X = 5 R_E, which contains the position of the cusps (diamonds) for a magnetopause standoff distance of 10 R_E. The reconnection conditions are satisfied along a merging line lying parallel to the ecliptic plane, the projection of which is indicated by the horizontal (dot-dashed) line. In this case the merging line length is limited to the arbitrary maximum of 8 R_E. Pairs of open reconnected flux tubes are initiated along the merging line (the central pair being at the originally selected location) and the motion of each tube is calculated as described in the text. The points of intersection of each tube with the magnetopause over a period of 500 s are plotted. The solid lines indicate the trajectories of tubes which connect to the northern cusp, and the dashed lines indicate those which connect to the southern cusp.

3.1. Southward IMF

In the example shown in Figure 6 we first examine the classical case of reconnection on the subsolar magnetopause for pure southward IMF of $(0, 0, -10)$nT, and we impose an initial reconnection location at the subsolar point itself. At this point the sheath flow velocity is zero as it is the stagnation point of the gasdynamic flow. The draped magnetosheath field at this point remains purely southward, and the geomagnetic field remains purely northward.

Considering first the pair of flux tubes formed by reconnection at the subsolar point itself, we find that the initial flux tube velocity is directly northward (southward) with a speed equal to that of the Alfvén speed. As these tubes move cuspward away from the subsolar point, the Alfvén

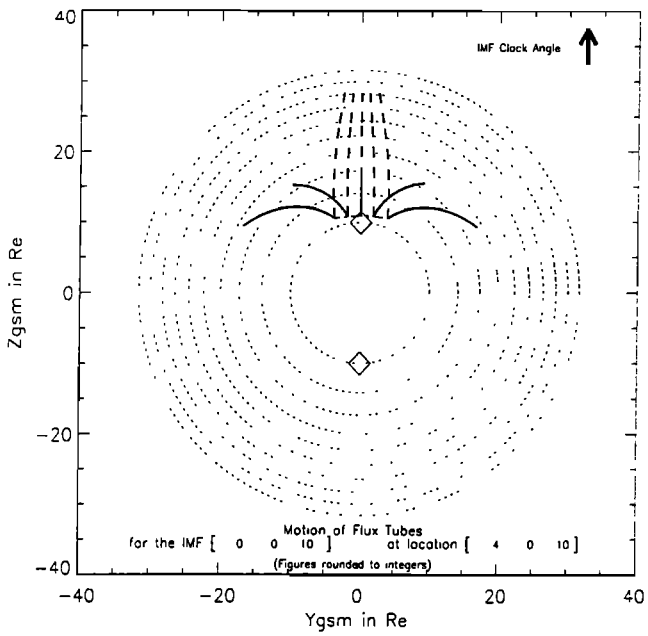

Figure 7. As in Figure 6 but for northward IMF. Flux tubes connected to the northern cusp (solid lines) move back over the merging line and also cross the path of reconnected flux tubes with both ends in the solar wind (dashed lines). Hence a steady state cannot be maintained in such a case.

speed changes, and the sheath flow increases. However, the sheath flow vector is also directly cuspward; thus the flux tubes accelerate toward the relevant cusps. This accords directly with the classical expectations for the motion of open flux tubes formed by the reconnection of a purely southward IMF at the subsolar point [e.g., *Dungey*, 1961].

Consider now a pair of open flux tubes formed by reconnection at a point on the merging line dawnward of the subsolar point. In this case the sheath flow will be non-zero and directed dawnward along the merging line. The initial motion of the flux tubes is thus northward (southward) away from the merging line and dawnward. As they recede from the merging line, they move into regions in which the sheath flow has an increasing poleward component. Additionally, the draped magnetosheath field has a dawnward (duskward) component in the Northern (Southern) Hemisphere. Changes in field strength and density also result in the flux tubes moving into regions of increased Alfvén speed. The overall effect is that these flux tubes accelerate into a more tailward direction as they unwind. In this case there is a dawn-dusk, north-south symmetry in the motion of reconnected flux tubes. Thus open windows develop over the magnetopause initially with the merging line width but expanding to a dawn-dusk width of around 15-20 R_E by the time the flux tubes have moved tailward to X =-5 R_E.

3.2. Northward IMF

We now present the results of two model runs for a pure northward IMF $(0, 0, 10)$nT. We show that if we use the standard velocity and density parameters in our calculations, then steady state reconnection poleward of the cusp under northward IMF is not predicted. We then show that if we reduce the density calculated in our model, then we can find steady state reconnection under these conditions.

We impose an initial reconnection location just poleward of the northern cusp where the magnetosheath and geomagnetic fields for pure northward IMF are exactly antiparallel; thus the current direction is dusk-dawn. In the first case, shown in Figure 7, the model is able to calculate flux tube paths for a reconnection event at this location, but the steady state test is not satisfied. The paths of the flux tubes connected to the northern cusp move back over the merging line. They also cross the path of reconnected flux tubes with both ends in the solar wind in this configuration. This is a consequence of the strong magnetosheath flow which is super-Alfvénic and directed tailward and parallel to the magnetosheath field in these regions. Since this result implies either a motion of the merging line or cessation of reconnection, this is impossible under steady state conditions. However, a transient burst of reconnection may occur at this point, since all other criteria are satisfied. The trajectories shown in Figure 7 then represent the paths that flux tubes formed in this manner are expected to follow.

In the example shown in Figure 8 we use the same IMF and reconnection location as above. However, we have arbitrarily reduced the density to 20% of the value arrived at from our Spreiter-derived model in section 2.6. The effect of reducing the density in this manner is to increase the Alfvén speed, such that the magnetosheath flow at the reconnection site is now just sub-Alfvénic. A similar effect may be

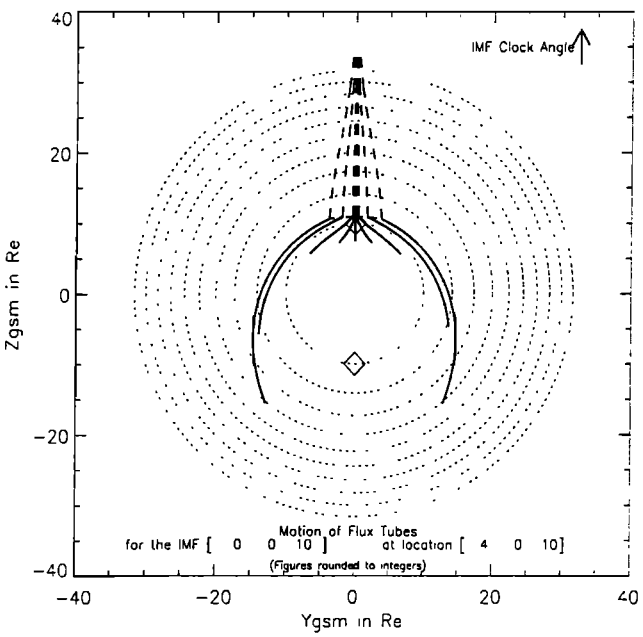

Figure 8. As in Figure 7 but with an arbitrary reduction in magnetosheath density to 20% of the value derived from the Spreiter gasdynamic model. The steady state condition is now satisfied. Note the very slow movement equatorward of the central north-connected tube.

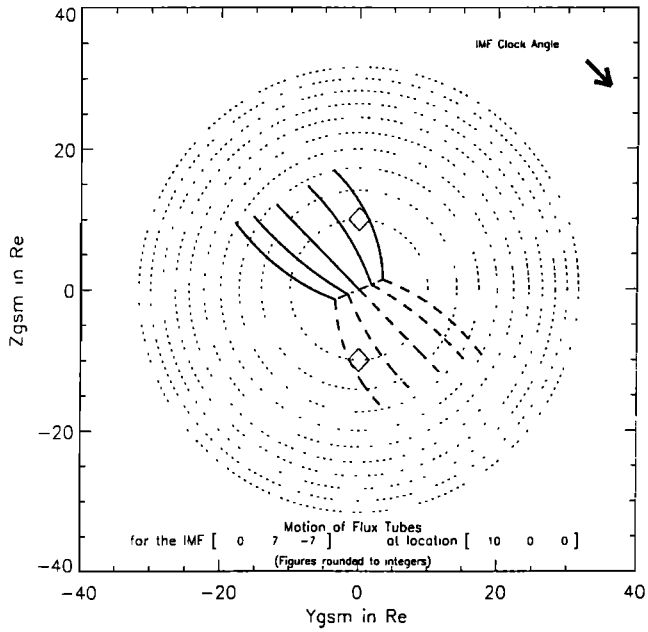

Figure 9. Flux tube motion following reconnection for an IMF of clock angle 135°. The tubes have a distinct dawn-dusk asymmetry to their motion. The tubes connected to the northern cusp (solid lines) move dawnward and behind the cusp, and those connected to the southern cusp (dashed lines) move duskward.

achieved by increasing the IMF strength or by reducing the speed derived from the Spreiter model. The steady state condition is now satisfied and accords with recent observations which suggest that a plasma depletion layer effect may allow quasi-steady reconnection tailward of the cusp under northward IMF [e.g., *Fuselier et al.*, 2000].

In particular, we note that the central tube connected to the northern cusp moves sunward very slowly under these conditions, $\sim 3\ R_E$ in around 500 s, as indicated by the short solid line. The motion of this central tube may be an artifact of our treatment of the cusp in the model; however, the tubes immediately adjacent to the cusp exhibit similar motion. The outermost north-cusp-connected open flux tubes move sharply southward down the flanks. The resulting open flux window, bound by the outermost tubes, is very broad and covers a large part of the dayside. The tailward window is quite narrow and extends directly antisunward. The reconnected flux tubes which map out into solar wind at both ends, now move tailward at around $2V_A$, double the sheath flow velocity. One consequence of this is that the boundary layer flows for these flux tubes are almost $3V_A$ in the Earth frame. These flows may correspond to the accelerated plasma flows on the magnetosheath side of the magnetopause observed by, for example, *Gosling et al.* [1986].

3.3. Southward IMF With Nonzero B_Y

In Figure 9 we show the flux tube motion for an IMF of clock angle 135°, $(0, 7, -7)$nT, with initial reconnection point again located at the subsolar point. The conditions for initial and steady state reconnection are once more met. The merging line passes through the subsolar point but is tilted out of the ecliptic plane. The draped magnetic field crossing the subsolar point retains its IMF orientation, and the central tubes move radially away from the subsolar point, parallel to the sheath flow, with the northern tube heading over to the dawnside and the southern tube heading toward dusk.

The outermost north-connected tube forms just below the ecliptic plane. Here the sheath flow is directed tailward and southward; however, its speed is still quite slow. The draped field has gained a slight duskward component, and the resulting initial motion of the tube is thus dominated by the velocity component antiparallel to the magnetosheath field. As the tube moves tailward, it moves into a region of greater radial sheath flow speed which, combined with the draping, begins to pull the tube toward and parallel to the central tube. The open window connected to the northern (southern) cusp broadens out over the dawn (dusk) sectors at high latitudes before narrowing off downtail. In this configuration, magnetic flux is added to the tail lobes in an asymmetrical manner.

3.4. Parker Spiral Fields With Northward B_Z

Here we show open flux tube motion for the two Parker spiral field directions with northward B_Z. We used the reduced density version of the model and initiated reconnection poleward of the northern cusp.

In Figure 10 we show the "away" sector configuration with the duskward B_Y component $(-6, 6, 6)$nT. The model returns a merging line running from high latitudes at the dawnward end to lower latitudes at the duskward ex-

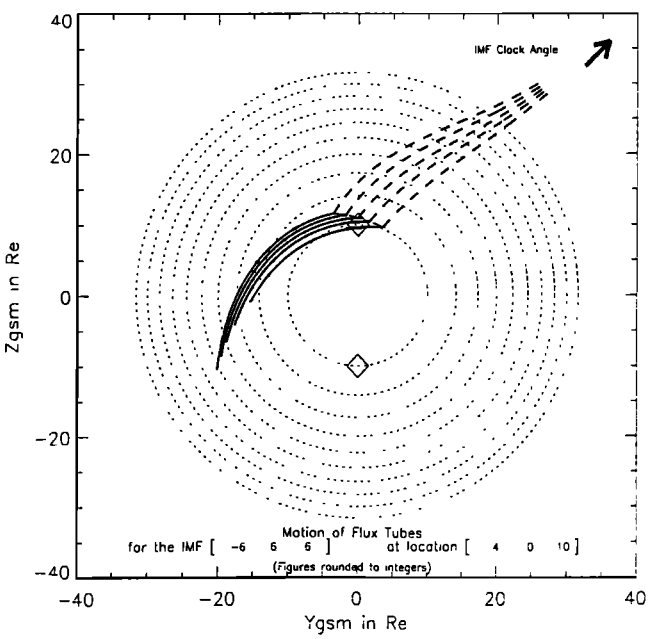

Figure 10. Flux tube motion after reconnection for "away" sector Parker spiral with northward B_Z IMF of (-6,6,6)nT using a reduced density of 20%. The result satisfies the steady state reconnection conditions.

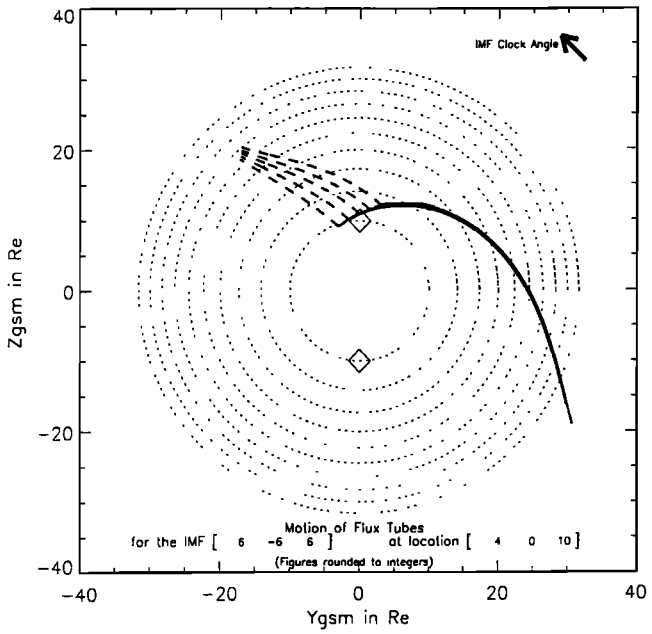

Figure 11. Flux tube motion after reconnection for "toward" sector Parker spiral with northward B_Z IMF of (6,-6,6)nT, also with reduced density. In this case the result only just satisfies the steady state reconnection condition. Note that this is not a reflection of Figure 10.

treme. The north-cusp-connected open window is quite narrow and stretches down and round the dawn flank. The flux tubes connected downtail (ultimately to interplanetary space) move faster, tailward, and duskward, forming an open window over the dusk quadrant of the northern lobe of the magnetotail.

The "toward" sector Parker spiral configuration with dawnward B_Y component $(6, -6, 6)$nT is shown in Figure 11. In this case the steady state condition is only just satisfied. The flux tubes connected to interplanetary space now move tailward over the dawn flank of the magnetopause, while the north-cusp-connected tubes move around the southern dusk flank. Note that this motion is not symmetric with the "away" sector case shown in Figure 10. The velocities of the IMF-connected flux tubes are somewhat slower than those in the "away" spiral case, and the tubes connected to the northern cusp are much faster, as evidenced by the relative length (distance traveled in 500 s) of the respective trajectories. The window formed by the latter flux tubes is extremely narrow.

3.5. Structure of the Sheath Flow

The results presented in Sections 3.2 - 3.4 emphasize the importance of the sheath flow in determining the motion of open flux tubes along the magnetopause. In particular, the value of the sheath flow Alfvén Mach number is critical in determining whether steady state reconnection may occur. To investigate this further, we have mapped the ratio $|\mathbf{V}_{sh}.\hat{\mathbf{q}}|/|V_A\mathbf{b}_{ms}.\hat{\mathbf{q}}|$ (see section 2.7.3) over the surface of the magnetopause. By way of example, consider the case of the "away" sector Parker spiral direction with northward B_Z component $(-6, 6, 6)$nT, shown in Figure 12, which uses the standard density model. We find that there is a band $\sim 3\ R_E$ (1 hour) wide stretching from cusp to cusp and centered on magnetic local time (MLT) noon where the ratio is less than 1 and hence the steady state condition is satisfied. There is a dawn-dusk asymmetry visible at both the cusps, with sub-Alfvénic flows only on the dusk-side (dawn-side) of the northern (southern) cusp. The region of sub-Alfvénic flow also extends to slightly higher latitudes in the Northern Hemisphere than it does in the Southern Hemisphere and has a broader duskward extension than the dawnward extension at the southern cusp. This effect becomes more marked when a reduced magnetosheath density is used. In this example the asymmetry is due to the different symmetries of the draped magnetosheath and the geomagnetic field, where the directional vector is symmetrical about the line $Y = 0$. We would expect therefore to see asymmetries in the convection patterns at the opposing polar caps.

4. Discussion

Our model represents a substantial extension to that of CO89. In particular, unlike CO89, who considered only the initial motion, we follow the evolution of the reconnected flux tube motion into the tail. To achieve this we use a more

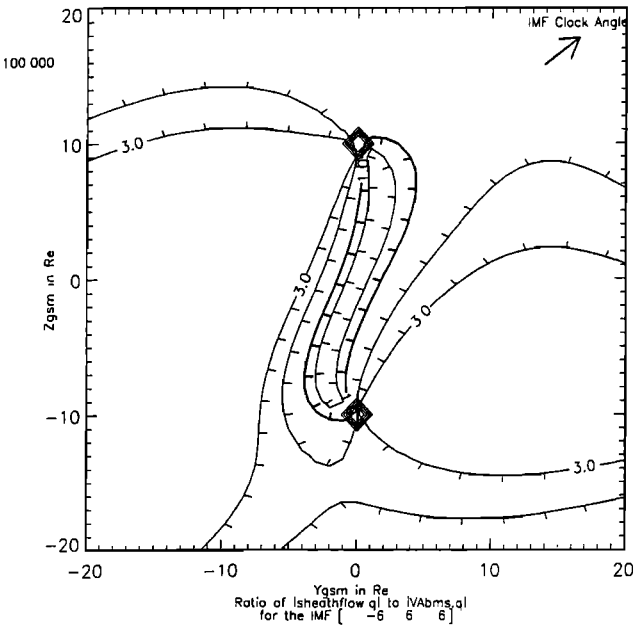

Figure 12. Contours showing the ratio $|\mathbf{V}_{sh}.\hat{\mathbf{q}}|/|V_A\mathbf{b}_{ms}.\hat{\mathbf{q}}|$ on a YZ projection of the magnetopause for an "away" Parker spiral with northward B_Z component (-6,6,6)nT and with standard density. The two shaded diamonds represent the cusps. The heavy contour shows the locations where the ratio is 1, and the short lines illustrate the decreasing edge of the contour. The elongated north-south sausage-shaped contour stretching between the cusps is the region where steady state reconnection for this IMF at 100% density may occur in our model.

realistic paraboloid shape to represent the magnetopause, rather than a plane. Additionally, we use a more realistic model of the draped magnetosheath field, together with a simple representation of the geomagnetic field. We also utilize *Spreiter et al.'s* [1966] gasdynamic sheath flow model. While each component on its own is not new, the way in which we have put the parts together is.

There are a number of assumptions both implicit and explicit in our model. However, these are reasonably representative of the real magnetopause, adequately reproducing, for example, expectations from the classical southward B_Z picture (Figure 6). The results can be regarded as semiquantitative while maintaining the advantage of not requiring large amounts of computing time. The model is suited therefore to rapid hypothesis testing.

Our model gives a clear picture of how the open flux windows may spread over the magnetopause and thus where magnetic flux is added to the magnetotail. Asymmetrical loading of flux (Figure 9) may, for example, give rise to net torques being applied to the magnetotail which may in turn cause tail twisting [*Cowley*, 1982; *Owen et al.*, 1995], or asymmetries in the plasma populations in the two tail lobes [*Gosling et al.*, 1982, 1986].

The asymmetry between the two Parker spiral orientations shown in Figures 10 and 11 will translate into the magnetosphere and down to the flux tube footpoints in the auroral ionosphere. Thus the ionospheric flow patterns should also show as a statistical asymmetry when sorted by IMF B_Y. This is characteristic of the Svalgaard-Mansurov effect [*Svalgaard*, 1968; *Mansurov*, 1969]. These authors independently discovered a correlation between the vertical components of the geomagnetic field and the B_Y component of the IMF, later suggesting [*Svalgaard*, 1973] that this may be caused by a narrow current circulating clockwise (anticlockwise) at the North Pole for negative (positive) B_Y and in the opposite direction at the South Pole. *Heppner* [1972] also observed correlations between B_Y and the dawn-dusk asymmetries of the polar electric field. These characteristics are consistent with the motion of open flux tubes across the magnetopause shown in Figures 9-11.

We have not explicitly considered the effects of dipole tilting in this paper. However, assuming that the magnetosheath flow and magnetic field parameters are unchanged by tilting, the example shown in Figure 12 and the results of section 3.5 show that very little, if any, sunward tilting of the dipole (northern summer) would be necessary to bring an initial reconnection site poleward of the northern cusp into the region of sub-Alfvénic flow and hence to satisfy the steady state condition. Antisunward tilting (northern winter) could bring the southern cusp into a sub-Alfvénic region provided that the initial reconnection site was offset to the dawnside. Seasonal asymmetries of polar cap convection currents have been seen by some observers [see *Kennel*, 1995, and references therein], and this work may contribute to an understanding of these phenomena.

Our results show the sensitivity of the model's predictions as to whether the magnetosheath flow is sub- or super-Alfvénic at the reconnection site. This is particularly important poleward of the cusps under northward IMF conditions. If the Spreiter model for magnetosheath flow is correct and flows poleward of the cusp are super-Alfvénic, then steady state reconnection under northward IMF is not possible in this region. The standard Spreiter model gives super-Alfvénic flow within 5 - 10 R_E of the sub-solar point [*Cowley*, 1995], i.e., well equatorward of the cusp.

In order to achieve steady state reconnection poleward of the cusps, a mechanism for producing sub-Alfvénic flow must be found. In our northward IMF examples (e.g., Figures 7 and 8) we achieved this by arbitrarily reducing the density to 20% of the value predicted by the Spreiter model in order to modify the Alfvén Mach number within the magnetosheath. Similar effects may be achieved by increasing the magnetosheath field strength at the magnetopause, by reducing the magnetosheath flow speed predicted by the Spreiter model, or a combination of all three.

A study of 20 events by *Crooker et al.* [1984] showed that only about half of the magnetosheath flows followed the gasdynamic predictions. A recent study by *Siscoe et al.* [2000] also shows deviation from the gasdynamic predictions. In addition, it was reported by *Alexeev et al.* [1998] that using the magnetosheath model of KF94 without a density depletion overestimated field magnitude. The density predicted by the Spreiter models may be too high, and a physical mechanism which reduces the plasma density in the vicinity of the magnetopause may be in operation [e.g., *Zwan and Wolf*, 1976; *Le et al.*, 1996].

5. Conclusions

We have constructed a model which follows open flux tube motion along the Earth's magnetopause after reconnection at a given location and for a given set of IMF conditions. We find the following: (1) The model reproduces the expected poleward motions of open field lines for southward B_Z. (2) For northward B_Z the model's predictions are very sensitive to whether the flows are sub- or super-Alfvénic for reconnection occuring poleward of the cusp. This indicates that work on comparing flow observations with model predictions would be useful in further investigations into signatures of reconnection in general and conditions for steady state reconnection under northward IMF in particular. (3) B_Y effects can lead to asymmetrical loading of the tail. (4) Flux tube motions for the two Parker spiral directions are asymmetrical and may thus explain statistical asymmetries in the dayside polar ionosphere convection patterns.

On the basis of northward IMF studies we conclude that steady state reconnection poleward of the cusp will not occur under typical conditions unless one or more of the magnetosheath flow, density, and field models are modified or unless dipole tilt is sufficient to bring the cusp into a sub-Alfvénic flow region. The model also helps identify the possible or most likely sites at which steady state reconnection will occur.

Acknowledgments. B.M.A.C. and C.J.O. are supported by a UK PPARC Studentship and Advanced Fellowship, respectively.

Janet G. Luhmann thanks Ronald K. Elsen, George L. Siscoe, and another referee for their assistance in evaluating this paper.

References

Alexeev, I. I., D. G. Sibeck, and S. Y. Bobrovnikov, Concerning the location of magnetopause merging as a function of the magnetopause current strength, *J. Geophys. Res., 103*, 6675–6684, 1998.

Alksne, A. Y., The steady-state magnetic field in the transition region between the magnetosphere and the bowshock, *Planet. Space Sci., 15*, 239–245, 1967.

Chen, S. H., S. A. Boardsen, S. F. Fung, J. L. Green, R. L. Kessel, L. C. Tan, T. E. Eastman, and J. D. Craven, Exterior and interior polar cusps: Observations from Hawkeye, *J. Geophys. Res., 102*, 11,335 – 11,347, 1997.

Coleman, I. J., M. Pinnock, and A. S. Rodger, The ionospheric footprint of antiparallel merging regions on the dayside magnetopause, *Ann. Geophys., 18*, 511 – 516, 2000.

Cowley, S. W. H., The formation and properties of boundary layers downstream from neutral lines in an open magnetosphere, in *Magnetospheric Boundary Layers*, edited by B. Battrick, Eur. Space Agency Spec. Publ. ESA SP-148, p. 333, 1979.

Cowley, S. W. H., Magnetospheric asymmetries associated with the Y-component of the IMF, *Planet. Space Sci., 29*, 79–96, 1981.

Cowley, S. W. H., The causes of convection within the Earth's magnetosphere: A review of developments during the IMS, *Rev. Geophys., 20*, 531–565, 1982.

Cowley, S. W. H., Theoretical perspectives of the magnetopause: A tutorial review, in *Physics of the Magnetopause, Geophys. Monogr. Ser.*, vol. 90, edited by P. Song, B. U. Ö. Sonnerup, and M. F. Thomsen, pp. 29–43, AGU, Washington, D. C., 1995.

Cowley, S. W. H., and C. J. Owen, A simple illustrative model of open flux tube motion over the dayside magnetopause, *Planet. Space Sci., 37*, 1461–1475, 1989.

Cowley, S. W. H., D. J. Southwood, and M. A. Saunders, Interpretation of magnetic field perturbations in the Earth's magnetopause boundary layers, *Planet. Space Sci., 31*, 1237–1258, 1983.

Crooker, N. U., Dayside merging and cusp geometry, *J. Geophys. Res., 84*, 951–959, 1979.

Crooker, N. U., A split separator line merging model of the dayside magnetopause, *J. Geophys. Res., 90*, 12,104–12,110, 1985.

Crooker, N. U., G. L. Siscoe, T. E. Eastman, L. A. Frank, and R. D. Zwickl, Large-scale flow in the dayside magnetosheath, *J. Geophys. Res., 89*, 9711–9719, 1984.

Crooker, N. U., J. G. Luhmann, C. T. Russell, E. J. Smith, J. R. Spreiter, and S. S. Stahara, Magnetic field draping against the dayside magnetopause, *J. Geophys. Res., 90*, 3505–3510, 1985.

Crooker, N. U., G. L. Siscoe, and F. R. Toffoletto, A tangent subsolar merging line, *J. Geophys. Res., 95*, 3787–3793, 1990.

de Hoffmann, F., and E. Teller, Magneto-hydrodynamic shocks, *Phys. Rev., 80*, 692, 1950.

Drakou, E., B. U. Ö. Sonnerup, and W. Lotko, Self-consistent steady-state model of the low-latitude boundary layer, *J. Geophys. Res., 99*, 2351 – 2364, 1994.

Dungey, J. W., Interplanetary field and the auroral zones, *Phys. Rev. Lett., 6*, 47–48, 1961.

Elsen, R. K., and R. M. Winglee, The average shape of the magnetopause: A comparison of three-dimensional global MHD and empirical models, *J. Geophys. Res., 102*, 4799–4819, 1997.

Fairfield, D. H., Structure of the magnetopause: Observations and implications for reconnection, *Space Sci. Rev., 23*, 427–448, 1979.

Fuselier, S. A., S. M. Petrinec, and K. J. Trattner, Stability of the high-latitude reconnection site for steady northward IMF, *Geophys. Res. Lett., 27*, 473–476, 2000.

Gonzalez, W. D., Comment on "A tangent subsolar merging line" by N. U. Crooker et al., *J. Geophys. Res., 96*, 1873–1874, 1991.

Gonzalez, W. D., and F. S. Mozer, A quantitative model for the potential resulting from reconnection with an arbitrary magnetic field, *J. Geophys. Res., 79*, 4186–4194, 1974.

Gosling, J. T., J. R. Asbridge, S. J. Bame, W. C. Feldman, G. Paschmann, N. Sckopke, and C. T. Russell, Evidence for quasi-steady reconnection at the dayside magnetopause, *J. Geophys. Res., 87*, 2147–2158, 1982.

Gosling, J. T., M. F. Thomsen, S. J. Bame, and C. T. Russell, Accelerated plasma flows at the near-tail magnetopause, *J. Geophys. Res., 91*, 3029–3041, 1986.

Gosling, J. T., M. F. Thomsen, S. J. Bame, R. C. Elphic, and C. T. Russell, Cold ion-beams in the low latitude boundary-layer during accelerated flow events, *Geophys. Res. Lett., 17*, 2245 – 2248, 1990.

Heikkila, W. J., Impulsive plasma transport through the magnetopause, *Geophys. Res. Lett., 9*, 159–162, 1982.

Heppner, J. P., Polar-cap electric field distributions related to the interplanetary magnetic field, *J. Geophys. Res., 77*, 4877–4887, 1972.

Kennel, C. F., *Convection and Substorms: Paradigms of Magnetospheric Phenomenology*, Int. Ser. Astron. Astrophys., Oxford Univ. Press, New York, 1995.

Kobel, E., and E. O. Flückiger, A model of the steady state magnetic field in the magnetosheath, *J. Geophys. Res., 99*, 23,617–23,622, 1994.

Konik, R. M., L. J. Lanzerotti, A. Wolfe, C. G. MacLennan, and D. Venkatesan, Cusp latitude magnetic impulse events, 2, Interplanetary magnetic field and solar wind conditions, *J. Geophys. Res., 99*, 14,831 – 14,853, 1994.

Korotova, G. I., and D. G. Sibeck, A case-study of transient event motion in the magnetosphere and in the ionosphere, *J. Geophys. Res., 100*, 35 – 46, 1995.

Le, G., C. T. Russell, J. T. Gosling, and M. F. Thomsen, ISEE observations of low-latitude boundary layer for northward interplanetary magnetic field: Implications for cusp reconnection, *J. Geophys. Res., 101*, 27,239–27,249, 1996.

Lockwood, M., Location and characteristics of the reconnection X-line deduced from low-altitude satellite and ground-based observations,1, Theory, *J. Geophys. Res., 100*, 21,791 – 21,802, 1995.

Lockwood, M., Energy and pitch-angle dispersions of LLBL/cusp ions seen at middle altitudes: Predictions by the open magnetosphere model, *Ann. Geophys., 15*, 1501 – 1514, 1997.

Lockwood, M., and C. J. Davis, Occurrence probability, width and number of steps of cusp precipitation for fully pulsed reconnection at the dayside magnetopause, *J. Geophys. Res., 100*, 7627 – 7640, 1995.

Lockwood, M., and M. F. Smith, Low and middle altitude cusp particle signatures for general magnetopause reconnection rate variations, 1, Theory, *J. Geophys. Res., 99*, 8531 – 8553, 1994.

Luhmann, J. G., R. J. Walker, C. T. Russell, N. U. Crooker, J. R. Spreiter, and S. S. Stahara, Patterns of potential magnetic field merging sites on the dayside magnetopause, *J. Geophys. Res., 89*, 1739–1742, 1984.

Mansurov, S. M., New evidence of a relationship between magnetic fields in space and on Earth, *Geomagn. Aeron., 4*, 768–770, 1969.

Mei, Y., N. U. Crooker, and G. L. Siscoe, Cusp currents from ionospheric vorticity generated by gasdynamic and merging flow-fields at the magnetopause, *J. Geophys. Res., 100*, 7641 – 7647, 1995.

Onsager, T. G., S. W. Chang, J. D. Perez, J. B. Austin, and L. X. Janoo, Low-altitude observations and modeling of quasi-steady magnetopause reconnection, *J. Geophys. Res., 100*, 11,831 – 11,843, 1995.

Owen, C. J., and S. W. H. Cowley, Heikkila mechanism for impul-

sive plasma transport through the magnetopause: A reexamination, *J. Geophys. Res.*, *96*, 5565 – 5574, 1991.

Owen, C. J., J. A. Slavin, I. G. Richardson, N. Murphy, and R. J. Hynds, Average motion, structure and orientation of the distant magnetotail determined from remote sensing of the edge of the plasma sheet boundary layer with E >35keV ions, *J. Geophys. Res.*, *100*, 185–204, 1995.

Parks, G. K., *Physics of Space Plasmas: An Introduction*, Addison-Wesley-Longman, Reading, Mass., 1991.

Petschek, H. E., Magnetic field annihilation, in *The Physics of Solar Flares*, edited by W. N. Hess, NASA Spec. Publ. SP-50, p. 425, 1964.

Pudovkin, M. I., and V. S. Semenov, Magnetic field reconnection theory and the solar wind - magnetosphere interaction: A review, *Space Sci. Rev.*, *41*, 1–89, 1985.

Rodger, A. S., I. J. Coleman, and M. Pinnock, Some comments on transient and steady-state reconnection at the dayside magnetopause, *Geophys. Res. Lett.*, *27*, 1359–1362, 2000.

Russell, C. T., and R. C. Elphic, ISEE observations of flux transfer events at the dayside magnetopause, *Geophys. Res. Lett.*, *6*, 33–36, 1979.

Siscoe, G. L., G. M. Erickson, B. U. Ö. Sonnerup, N. C. Maynard, K. D. Siebert, D. R. Weimer, and W. W. White, Deflected magnetosheath flow at the high-latitude magnetopause, *J. Geophys. Res.*, *105*, 12,851 – 12,857, 2000.

Song, P., and C. T. Russell, Model of the formation of the low-latitude boundary layer for strongly northward interplanetary magnetic field, *J. Geophys. Res.*, *97*, 1411 – 1420, 1992.

Sonnerup, B. U. Ö., Transport mechanisms at the magnetopause, in *Dynamics of the Magnetosphere*, edited by S.-I. Akasofu, p. 77, D. Reidel, Norwell, Mass., 1979.

Sonnerup, B. U. Ö., G. Paschmann, I. Papamastorakis, N. Sckopke, G. Haerendel, S. J. Bame, J. R. Asbridge, J. T. Gosling, and C. T. Russell, Evidence for magnetic field reconnection at the Earth's magnetopause, *J. Geophys. Res.*, *86*, 10,049–10,067, 1981.

Spreiter, J. R., A. L. Summers, and A. Y. Alksne, Hydromagnetic flow around the magnetosphere, *Planet. Space Sci.*, *14*, 223–253, 1966.

Stern, D. P., A study of the electric field in an open magnetospheric model, *J. Geophys. Res.*, *78*, 7292–7305, 1973.

Svalgaard, L., Sector structure of the interplanetary magnetic field and daily variation of the geomagnetic field at high latitudes, *Geophys. Pap. R-6*, Dan. Meteorol. Inst., Copenhagen, 1968.

Svalgaard, L., Polar cap magnetic variations and their relationship with the interplanetary magnetic sector structure, *J. Geophys. Res.*, *78*, 2064–2078, 1973.

Taguchi, S., M. Sugiura, J. D. Winningham, and J. A. Slavin, Characterization of the IMF B_y -dependent field-aligned currents in the cleft region based on DE -2 observations, *J. Geophys. Res.*, *98*, 1393 – 1407, 1993.

Tsyganenko, N. A., Modeling the Earth's magnetospheric magnetic field confined within a realistic magnetopause, *J. Geophys. Res.*, *100*, 5599–5612, 1995.

Zwan, B. J., and R. A. Wolf, Depletion of solar wind plasma near a boundary layer, *J. Geophys. Res.*, *81*, 1636–1648, 1976.

B. M. A. Cooling and S. J. Schwartz, Astronomy Unit, Queen Mary, University of London, Mile End Road, London E1 4NS, England, UK. (b.cooling@qmw.ac.uk; s.j.schwartz@qmw.ac.uk)

C. J. Owen, Mullard Space Science Laboratory, University College London, Holmbury St. Mary, Dorking RH5 6NT, England, UK. (cjo@mssl.ucl.ac.uk)

(Received December 8, 2000; revised March 19, 2001;
accepted March 19, 2001.)